Published in final edited form as:
Clin Biomech (Bristol, Avon). 2013 April ; 28(4): 402–407. doi:10.1016/j.clinbiomech.2013.02.014.

Narrowing carpal arch width to increase cross-sectional area of carpal tunnel – a cadaveric study

Zong-Ming Li, **Joseph N. Gabra**, **Tamara L. Marquardt**, and **Dong Hee Kim**
Hand Research Laboratory, Departments of Biomedical Engineering, Orthopaedic Surgery, and Physical Medicine and Rehabilitation, Cleveland Clinic, Cleveland, Ohio, USA

Abstract

Background—Carpal tunnel morphology plays an essential role in the etiology and treatment of carpal tunnel syndrome. The purpose of this study was to observe the morphological changes of the carpal tunnel as a result of carpal arch width narrowing. It was hypothesized carpal arch width narrowing would result in increased height and area of the carpal arch.

Methods—The carpal arch width of eight cadaveric hands was narrowed by a custom apparatus and cross-sectional ultrasound images were acquired. The carpal arch height and area were quantified as the carpal arch width was narrowed. Correlation and regression analyses were performed for the carpal arch height and area with respect to the carpal arch width.

Findings—The carpal tunnel became more convex as the carpal arch width was narrowed. The initial carpal arch width, height, and area were 25.7 (SD 1.9) mm, 4.1 (SD 0.6) mm, and 68.5 (SD 14.0) mm^2, respectively. The carpal arch height and area negatively correlated with the carpal arch width, with correlation coefficients of −0.974 (SD 0.018) and −0.925 (SD 0.034), respectively. Linear regression analyses showed a 1 mm narrowing of the carpal arch width resulted in proportional increases of 0.40 (SD 0.14) mm in the carpal arch height and 4.0 (SD 2.2) mm^2 in the carpal arch area.

Interpretation—This study demonstrates that carpal arch width narrowing leads to increased carpal arch height and area, a potential mechanism to reduce the mechanical insult to the median nerve and relieve symptoms associated with carpal tunnel syndrome.

Keywords

Carpal arch; carpal tunnel; width; height; area

Introduction

The carpal tunnel is a unique fibro-osseous structure formed by the transverse carpal ligament at the palmar side and by the carpal bones at the dorsal, the radial and the ulnar aspects. Within the tunnel, the nine flexor tendons and the median nerve traverse through the confined space. Many etiological factors may contribute to the compression of the median nerve in the tunnel, leading to the prevalent hand disorder called carpal tunnel syndrome

Correspondence: Zong-Ming Li, PhD, Cleveland Clinic, 9500 Euclid Avenue, ND20, Cleveland, OH 44195, Phone: (216) 444-1211, Fax: (216) 444-9198, liz4@ccf.org.

(Moore, 2002). Routinely, carpal tunnel release is performed, whereby the transverse carpal ligament is transected in a surgical procedure to decompress the median nerve and relieve the symptoms of carpal tunnel syndrome. However, surgical release of the ligament compromises biomechanical integrity of the carpal tunnel, causing a number of post-operative complications such as weakness of grip strength, pillar pain and recurrence of symptoms (Fuss and Wagner, 1996, Kline and Moore, 1992). Many non-operative procedures for the intervention of carpal tunnel system have been attempted, but their long-term efficacy is lacking (Huisstede et al., 2010).

Carpal tunnel morphology plays an essential role in the etiology and treatment of carpal tunnel syndrome (Bekkelund and Pierre-Jerome, 2003, Kato et al., 1994). The morphological characteristics of the tunnel have been extensively studied using a variety of techniques including (i) radiography (Cobb et al., 1993, Gartsman et al., 1986, Viegas et al., 1992), (ii) computed tomography (Bleecker et al., 1985, Flores et al., 2009, Jessurun et al., 1987), (iii) magnetic resonance imaging (Tsujii et al., 2009, Allmann et al., 1997, Mogk and Keir, 2007, Mesgarzadeh et al., 1989a), (iv) ultrasonography (Kamolz et al., 2001, Lee et al., 2005, Altinok and Karakas, 2004, Sarria et al., 2000), (v) plastination (Sora and Genser-Strobl, 2005) and (vi) molding (Pacek et al., 2010, Richman et al., 1987). Among the morphological parameters, a small cross-sectional area of the carpal tunnel (i.e. tunnel stenosis) has been considered to be a predisposing factor for idiopathic carpal tunnel syndrome because a small carpal tunnel provides less space for its contents (Cobb et al., 1997, Dekel et al., 1980, Bekkelund and Pierre-Jerome, 2003, Bleecker et al., 1985). As an anatomical structure with a soft tissue component, the carpal tunnel has some degree of compliance as shown in human and animal *in vitro* studies (Li et al., 2011, Tung et al., 2010). Clinical studies have shown that individuals with carpal tunnel syndrome have increased palmar bowing of the transverse carpal ligament (Buchberger et al., 1992, Mesgarzadeh et al., 1989b, Uchiyama et al., 2005, Allmann et al., 1997, Tsujii et al., 2009), presumably due to elevated carpal tunnel pressure (Goss and Agee, 2010, Gelberman et al., 1981). Carpal tunnel release surgery is known to increase carpal tunnel cross-sectional area and volume (Brooks et al., 2003, Richman et al., 1989, Ablove et al., 1994, Kato et al., 1994), which is correlated with a decrease in carpal tunnel pressure after the surgery (Gelberman et al., 1981, Okutsu et al., 1989). In a cadaveric study, the pressure-morphology relationship for a released carpal tunnel revealed a nine times greater compliance than that of a carpal tunnel with an intact transverse carpal ligament (Kim et al., 2013). This helps explain the reduction of carpal tunnel pressure and relief of symptoms for patients after carpal tunnel release surgery. Carpal tunnel release also leads to a change in the carpal arch width (CAW), measured between the trapezium and the hook of the hamate (Gartsman et al., 1986, Viegas et al., 1992). The CAW was also shown to vary when the wrist was flexed or extended from the neutral position (Garcia-Elias et al., 1992).

Recent studies have suggested an alternative mechanism to increase the carpal tunnel area by narrowing the CAW (Li et al., 2009, Li et al., 2011, Kim et al., 2013). When a force was applied from within the tunnel to the transverse carpal ligament in the palmar direction, the ligament insertion sites moved toward each other and the CAW was decreased (Li et al., 2009). This led to palmar bowing of the transverse carpal ligament and increases in the carpal arch height (CAH) and the carpal arch area (CAA). Additionally, it was shown that inter-carpal joint mobility provides flexibility for CAW narrowing (Gabra et al., 2012, Li et al., 2009), leading to carpal arch formation which benefits the carpal tunnel environment by accommodating physiological variations of pressure in the tunnel. Also, a study examining the morphological changes of the carpal tunnel in response to the carpal tunnel pressure showed that an increase in the tunnel pressure is associated with a decrease in the CAW and an increase in the tunnel circularity, contributing to an increase in the carpal tunnel area (Li et al., 2011). When the transverse carpal ligament was transected, the pressure increase

inside the carpal tunnel led to a decrease in the CAW and separation of the transected edges of the ligament, jointly contributing to the increase of the cross-sectional area (Kim et al., 2013). A geometric model to examine the relationship among the morphological parameters also showed that an increase in the carpal arch area was sensitive to CAW narrowing as well as lengthening of the transverse carpal ligament (Li et al., 2009). Furthermore, the *in vivo* biomechanical interaction of the thenar muscles and the transverse carpal ligament induced by isometric tip pinch was shown to be associated with an increased palmar bowing, a decreased CAW and an increased CAA (Shen and Li, 2013).

While previous studies showed the association of the carpal arch width and the carpal tunnel cross-sectional area, there is no study that directly controlled CAW narrowing and observed its morphological effect, particularly in regards to palmar bowing and the carpal tunnel area. As such, the purpose of this study was to examine the changes in the carpal tunnel cross section as a result of CAW narrowing using a cadaveric model. The cross section of the carpal tunnel was recorded by ultrasound imaging while the CAW was manipulated. The carpal arch formed by the transverse carpal ligament was analyzed on the ultrasound images. It was hypothesized that CAW narrowing would lead to greater palmar bowing with increases in the CAH and the CAA.

Methods

Preparation of cadaveric specimens

Eight (n = 8) fresh frozen cadaveric hand specimens [7 male, 1 female; 7 left, 1 right; age 54.6 (SD 5.9) years] were used in this study. The specimens were thawed overnight at room temperature prior to experimentation. To prepare each specimen, the palmar skin from 15 mm proximal to the distal wrist crease to the mid-palm was excised, and the remaining fat and fascia tissue superficial to the transverse carpal ligament was removed. Then, the carpal tunnel was evacuated by removing the flexor tendons and the median nerve. The hamate and the trapezium bones were identified at the palmar side of the wrist and a wire-lockable socket head cap screw (McMaster Carr, Aurora, OH, USA) was drilled into the hamate and the trapezium in the palmar to dorsal direction approximately 10 mm deep.

Apparatus for carpal arch narrowing

The narrowing of the CAW was implemented with a custom compressive apparatus (Figure 1A). The apparatus consisted of a base, two point steel-tipped probes (McMaster Carr, Aurora, OH, USA), and two orthopaedic MiniRail fixators (Orthofix Holdings, INC, Lewisville, TX, USA). The probes and the fixators were each attached to opposite sides of the base. The device provided positioning flexibility of the probes by translations and rotations.

Experimental Procedures

Following specimen preparation, a water-filled pressure balloon attached to a tube was inserted into the evacuated carpal tunnel and centered with respect to the tunnel's longitudinal axis. The balloon and tube were part of a custom pressure regulating system designed to regulate carpal tunnel pressure (Li et al., 2011). The balloon ends extended beyond the proximal and the distal edges of the transverse carpal ligament. Each specimen was positioned in a supinated, anatomically neutral position within a splint that was affixed to the compressive apparatus using Velcro (Figure 1A). The probes of the device were aligned with the pre-drilled holes in the cap screw heads so that the tip of each probe made point contact with the screw. Furthermore, the probes and fixators were adjusted to ensure that the CAW narrowing occurred along the line connecting the hook of hamate and ridge of the trapezium. The probes and fixators were rigidly fixed when the desired position and

orientation were achieved. The CAW was narrowed through a translator by turning a socket bit connected to the radial fixator on the trapezium side of the specimen (Figure 1A). The ulnar probe was kept in a locked position to allow the change of carpal arch width by the advancement of the radial probe.

The specimen and the apparatus were submerged in a tank of room temperature water for ultrasound imaging (Figure 1B). A linear array 18L6 HD transducer was affixed to a robotic arm (Denso Corp., Kariya, Aichi, Japan) and the transducer was manually navigated to transversely align along the level of the hook of the hamate and the ridge of the trapezium. A vertical distance of approximately 15 mm between the ultrasound transducer and the palmar side of the specimen was maintained to provide a water interface media for ultrasound imaging and to prevent the transducer from contacting the specimen during experimentation. After positioning the ultrasound transducer, the pressure of the balloon within the carpal tunnel was set and maintained at a simulated physiological pressure of 24 mmHg throughout the entire experiment (Seradge et al., 1995) using the custom pressure regulating system (Li et al., 2011). A constant pressure was chosen to isolate the analyses of the geometrical relationship without implicating the pressure effect on morphological changes (Li et al., 2011, Kim et al., 2013). To narrow the CAW, the probe on the trapezium side of the specimen was advanced by turning the socket bit 10 times, each time corresponding to a half-turn. The amount of CAW change did not necessarily correspond to the probe advancement, and the total amount of CAW narrowing was 3–5 mm. At each step, a cross-sectional image was captured by an ultrasound system (Acuson S2000, Siemens Medical Solutions USA, Inc., Mountain View, CA, USA). During ultrasound imaging, the ultrasound system was operated in 2D mode with tissue harmonic imaging and tissue equalization. The imaging frequency was 12 MHz and the depth of the image field was 4.5 cm.

Data Analysis

The translator used to advance the compression probe provided a controlled narrowing of the CAW in incremental steps, but the actual amount of CAW narrowing was variable among the specimens. The CAW at each incremental narrowing was determined based on bony landmarks, i.e. the most palmar aspects of the trapezium and the hamate. An in-house custom program developed with LabVIEW (National Instruments, Austin, TX, USA) was used to automatically track specific carpal tunnel landmarks (Shen and Li, 2012, Shen and Li, 2013, Kim et al., 2013). On the initial image (i.e. 0.0 mm of CAW narrowing), two region-of-interest boxes were created with the centroid of each box located at the most palmar aspect of the hook of the hamate and the ridge of the trapezium, respectively. The boxes were tracked using the pixel intensity within the defined regions of interest throughout the remaining images captured of the CAW narrowing. The coordinates of the centroids of the region-of-interest boxes were used to define the CAW and to calculate the amount of CAW narrowing. Then, the palmar boundary of the transverse carpal ligament was manually traced, with the *ImageJ* (v1.43, National Institutes of Health, USA) multi-point selection tool, to obtain its coordinates. Using the coordinates of the hook of the hamate, the ridge of the trapezium, and the boundary of the transverse carpal ligament, an in-house custom *MATLAB* (Mathworks, Natick, MA, USA) program was used to calculate the CAH and the CAA. The program rotated the coordinates so that the line connecting the hook of the hamate and the ridge of the trapezium served as the x-axis and the y-axis was found as the perpendicular bisector. The coordinates of the ligament boundary were fit with a polynomial function from the hook of the hamate to the ridge of the trapezium (Shen and Li, 2012). The CAH was defined as the greatest y-coordinate of the ligament curve, i.e. the perpendicular distance from the palmar apex of the ligament curve to the line of the CAW. The CAA was calculated as the integral of the ligament curve along and within the CAW. Pearson's

correlation and regression analyses were performed to examine the CAW-CAH and CAW-CAA relationships.

Results

These same bony landmarks (the most palmar aspects of the trapezium and the hamate) were consistently tracked on ultrasound images at various CAW narrowing conditions (Figure 2). As the CAW was narrowed, the cross section of the carpal tunnel changed from an oval shape to a more rounded shape (Figure 2), which was caused by the bowing of the transverse carpal ligament in the palmar direction (Figure 3).

The specimens had an initial CAW range from 21.9 mm to 27.9 mm and an average CAW of 25.7 (SD 1.9) mm. The initial CAH was also variable from 3.3 to 5.4 mm, with an average of 4.1 (SD 0.6) mm. The variable initial CAW and initial CAH led to a variable CAA ranging from 51.9 to 88.8 mm^2, with an average of 68.5 (SD 14.0) mm^2. Figure 4 and Figure 5 show the changes in the CAH and the CAA, respectively, in response to CAW narrowing for the 8 individual specimens. Despite the initial differences in the CAWs of the specimens, each specimen consistently showed the pattern that narrowing the CAW increased the CAH (Figure 4) and increased the CAA (Figure 5).

The CAH and the CAA were negatively correlated with the CAW, with correlation coefficients of −0.974 (SD 0.018) and −0.925 (SD 0.034), respectively. Therefore, linear regressions were applied to quantify the CAW-CAH and CAW-CAA relationships (Table 1). Regression analyses of the CAW vs. CAH showed an R^2-value of 0.940 (SD 0.057). The slope of the regression line was −0.402 (SD 0.138, range from −0.206 to −0.581), indicating that a decrease of 1 mm in the CAW caused an average increase of 0.402 mm in the CAH ($P < 0.001$). Regression analyses of the CAW vs. CAA revealed an R^2-value of 0.865 (SD 0.068) with a slope of −4.033 (SD 2.187, range from −1.793 to −8.412), indicating that a decrease of 1 mm in the CAW caused an average increase of 4.033 mm^2 in the CAA ($P < 0.001$). The slopes for the CAH or the CAA were variable for individual specimens (Table 1) due to their different initial CAWs and CAHs.

Discussion

In this study, the change of the carpal tunnel morphology in response to narrowing the CAW was examined. Utilizing cadaveric hand specimens, the change in the CAW was controlled by a narrowing apparatus and the corresponding cross-sectional ultrasound images were recorded. A carpal tunnel pressure of 24 mmHg was maintained to simulate physiological pressure in the carpal tunnel, which enabled the carpal tunnel to maintain its convexity while the CAW was narrowed. Submerging the specimens in water for non-contact ultrasound imaging allowed the carpal arch to deform without mechanical interference between the palmar wrist and the ultrasound probe. Ultrasonography has been shown to be a reliable imaging modality to examine the morphological parameters of the carpal tunnel (Kim et al., 2013, Shen and Li, 2013, Shen and Li, 2012, Kamolz et al., 2001, Sarria et al., 2000).

In previous studies, the morphological parameters of the carpal tunnel were investigated with respect to a force applied to the transverse carpal ligament from inside the tunnel (Li et al., 2009), a pressure applied within the carpal tunnel (Li et al., 2011, Kim et al., 2013), a biomechanical interaction between the thenar muscles and the transverse carpal ligament (Shen and Li, 2013), and a geometrical model (Li et al., 2009). While previous studies showed that an increase in the carpal tunnel area is associated with a decrease in the CAW (Li et al., 2011, Li et al., 2009, Kim et al., 2013, Shen and Li, 2013), the current study

demonstrates the causal effect of the CAW on carpal tunnel expansion by directly manipulating the width of the carpal arch and observing the corresponding deformation.

In the current study, a 1 mm narrowing of the CAW resulted in an increase of 0.4 mm in the CAH and an increase of 4.0 mm^2 in the CAA. The current results agree well with an *in vivo* study which showed that maximal isometric pinch is associated with a decrease of 0.8 mm in the CAW, an increase of 0.5 mm in the CAH and an increase of 5.1 mm^2 in the CAA (Shen and Li, 2013). However, the amount of increases in the CAH and the CAA in response to CAW narrowing were smaller than some previously reported (Li et al., 2009, Kim et al., 2013). When force was applied to the transverse carpal ligament, a decrease of 0.7 mm in the CAW, an increase of 1.7 mm in the CAH and an increase of 15.4 mm^2 in the CAA was shown as the force application increased from 10 N to 200 N (Li et al., 2009). When the carpal tunnel pressure was increased to 200 mmHg, the CAW decreased by 0.6 mm and the CAA increased by 13.3 mm^2 (Li et al., 2011). For a carpal tunnel with a transected transverse carpal ligament, a pressure application of 120 mmHg caused a decrease of 0.5 mm in the CAW, an increase of 0.9 mm in the carpal arch length, an increase of 3.5 mm in the CAH, and an increase of 56.0 mm^2 in the CAA (Kim et al., 2013).

These differences can be explained by several factors. First, the morphological change of the carpal tunnel is strongly dependent on the initial CAH. For a given amount of CAW narrowing, the carpal arch would gain greater increases in the CAH and the CAA for a flat carpal arch (i.e. no initial CAH) than that for an arched carpal tunnel (i.e. with an initial CAH). A geometrical model showed that if there is no initial CAH, a small decrease of 0.2 mm in the CAW will cause large increases of 1.5 mm in the CAH and of 16.1 mm^2 in the CAA (Li et al., 2009). However, it has been shown that the transverse carpal ligament has palmar bowing in the physiological and the pathophysiological conditions (Allmann et al., 1997, Mesgarzadeh et al., 1989a). Therefore, the consistency between the current results and the findings from an *in vivo* study (Shen and Li, 2013) could be explained by the fact that a constant pressure was applied to the tunnel to simulate the physiological environment (Seradge et al., 1995). Second, increases in the carpal arch length, together with CAW narrowing, contributed to increases in the CAH and the CAA (Li et al., 2009). The large increases in the CAH and the CAA in the study of released carpal tunnel could be accounted for by the pressure-induced separation of the transected ligament edges, increasing the effective length of the carpal arch and therefore the carpal arch area (Kim et al., 2013, Kato et al., 1994, Richman et al., 1989). The third explanation pertains to the different loading conditions on the carpal tunnel that have different biomechanical effects. In the current study, the carpal tunnel was deformed by point forces applied to the carpal bones, while the loading conditions in the previous studies were created by carpal tunnel pressure ((Li et al., 2011, Kim et al., 2013), force application directly to the ligament (Li et al., 2009) and contraction force of the thenar muscles (Shen and Li, 2013).

One limitation of this study is that only the palmar arch portion of the carpal tunnel was examined without the inclusion of the bony portion. The ultrasound images render clear anatomical boundaries at the palmar aspect of the carpal tunnel (Buchberger et al., 1992), but the tunnel outlines at the dorsal aspect are less definite due to acoustic shadowing of the carpal bones. Previous *in vivo* (Kato et al., 1994, Uchiyama et al., 2005), *in vitro* (Li et al., 2009, Li et al., 2011) and modeling (Li et al., 2009) studies showed that the palmar carpal arch is the dominant contributor to the change in the carpal tunnel area, while the area of the bony portion of the carpal tunnel remains relatively constant. For example, Kato et al. reported that endoscopic carpal tunnel release led to an increase in the carpal tunnel cross-sectional area by 88 mm^2, and most (82 mm^2, 93%) of the change was due to the increased palmar arch. Therefore, the relative change in the CAA reported in this study is indicative of the area change of the entire tunnel.

Another limitation of this study is that the palmar boundary of the transverse carpal ligament was chosen to calculate the CAH and the CAA because the exposed palmar aspect of the ligament produced a distinct tissue-water interface in the ultrasound images. The inclusion of the transverse carpal ligament tissue resulted in an over-estimation of the amount of space available to the carpal tunnel contents. For example, the initial CAH was on average 4.1 mm, but this is greater than the amount of palmar bowing of about 2–3 mm reported in the literature (Buchberger et al., 1992, Allmann et al., 1997, Altinok and Karakas, 2004). The greater CAH might be caused by the dissection preparation to remove tissues palmar to the transverse carpal ligament, lessening the constraint for palmar bowing. Similarly, the area available for the carpal tunnel contents within the palmar arch could be estimated by deducting the cross-sectional area of the transverse carpal ligament from the stated CAA values. Nonetheless, this bias of a constant value did not affect the pattern of the relative changes (see also (Kim et al., 2013). The slopes of the regression lines were indicative of the relative changes in the CAH or the CAA, and therefore were not affected by the constant amount of tissue height or area.

Lastly, this study is a geometrical consideration of the relationship among the CAW, the CAH and the CAA. The force applied to the carpal bones to achieve the desired CAW narrowing was not considered. A previous study showed that two pairs of 10 N forces applied to the proximal and distal levels of the carpal tunnel generated a CAW narrowing of 2.9 mm at the distal level and 11.2 mm at the proximal level (Xiu et al., 2010). Therefore, the 3 mm CAW narrowing in the current study is attainable with moderate force application.

In summary, we investigated the increases in the CAH and the CAA from well controlled CAW narrowing using cadaveric hands. Ultrasound imaging allows for the reliable examination of the carpal tunnel morphological parameters during biomechanical experimentation. As the CAW was shortened, the cross section of the carpal tunnel changed from an oval shape to a more rounded shape by palmar bowing of the transverse carpal ligament. The CAH and the CAA were consistently increased in response to CAW narrowing. A decrease of 1 mm in the CAW caused an average increase of 0.4 mm in the CAH and 4.0 mm^2 in the CAA, though the rates of increase for individual specimens were somewhat variable depending on the initial bowing condition of the carpal arch. This study suggests that the carpal tunnel can be geometrically manipulated to increase its cross-sectional area. In individuals with carpal tunnel syndrome, such an increase in the tunnel area may potentially decompress the median nerve and relieve the symptoms of carpal tunnel syndrome. Future studies are needed to investigate the strategy of CAW narrowing and the resulting carpal arch bowing and area expansion *in vivo*.

Acknowledgments

The authors acknowledge the support by National Institutes of Health (NIH/NIAMS R21AR062753).

References

Ablove RH, Peimer CA, Diao E, Oliverio R, Kuhn JP. Morphologic changes following endoscopic and two-portal subcutaneous carpal tunnel release. J Hand Surg [Am]. 1994; 19:821–6.

Allmann KH, Horch R, Uhl M, Gufler H, Altehoefer C, Stark GB, Langer M. MR imaging of the carpal tunnel. Eur J Radiol. 1997; 25:141–5. [PubMed: 9283842]

Altinok T, Karakas HM. Ultrasonographic evaluation of age-related changes in bowing of the flexor retinaculum. Surg Radiol Anat. 2004; 26:501–3. [PubMed: 15378278]

Bekkelund SI, Pierre-Jerome C. Does carpal canal stenosis predict outcome in women with carpal tunnel syndrome? Acta Neurol Scand. 2003; 107:102–5. [PubMed: 12580858]

Bleecker ML, Bohlman M, Moreland R, Tipton A. Carpal tunnel syndrome: role of carpal canal size. Neurology. 1985; 35:1599–604. [PubMed: 4058749]

Brooks JJ, Schiller JR, Allen SD, Akelman E. Biomechanical and anatomical consequences of carpal tunnel release. Clin Biomech (Bristol, Avon). 2003; 18:685–93.

Buchberger W, Judmaier W, Birbamer G, Lener M, Schmidauer C. Carpal tunnel syndrome: diagnosis with high-resolution sonography. AJR Am J Roentgenol. 1992; 159:793–8. [PubMed: 1529845]

Cobb TK, Bond JR, Cooney WP, Metcalf BJ. Assessment of the ratio of carpal contents to carpal tunnel volume in patients with carpal tunnel syndrome: a preliminary report. J Hand Surg [Am]. 1997; 22:635–9.

Cobb TK, Dalley BK, Posteraro RH, Lewis RC. Anatomy of the flexor retinaculum. J Hand Surg [Am]. 1993; 18:91–9.

Dekel S, Papaioannou T, Rushworth G, Coates R. Idiopathic carpal tunnel syndrome caused by carpal stenosis. Br Med J. 1980; 280:1297–9. [PubMed: 7388516]

Flores LP, Cavalcante TF, Neto OR, Alcantara FS. Quantitative analysis of the variation in angles of the carpal arch after open and endoscopic carpal tunnel release. Clinical article. J Neurosurg. 2009; 111:311–6. [PubMed: 19199454]

Fuss FK, Wagner TF. Biomechanical alterations in the carpal arch and hand muscles after carpal tunnel release: a further approach toward understanding the function of the flexor retinaculum and the cause of postoperative grip weakness. Clin Anat. 1996; 9:100–8. [PubMed: 8720784]

Gabra JN, Domalain M, Li ZM. Movement of the distal carpal row during narrowing and widening of the carpal arch width. J Biomech Eng. 2012; 134:101004. [PubMed: 23083195]

Garcia-Elias M, Sanchez-Freijo JM, Salo JM, Lluch AL. Dynamic changes of the transverse carpal arch during flexion-extension of the wrist: effects of sectioning the transverse carpal ligament. J Hand Surg [Am]. 1992; 17:1017–9.

Gartsman GM, Kovach JC, Crouch CC, Noble PC, Bennett JB. Carpal arch alteration after carpal tunnel release. J Hand Surg [Am]. 1986; 11:372–4.

Gelberman RH, Hergenroeder PT, Hargens AR, Lundborg GN, Akeson WH. The carpal tunnel syndrome. A study of carpal canal pressures. J Bone Joint Surg Am. 1981; 63:380–3. [PubMed: 7204435]

Goss BC, Agee JM. Dynamics of intracarpal tunnel pressure in patients with carpal tunnel syndrome. J Hand Surg Am. 2010; 35:197–206. [PubMed: 20022712]

Huisstede BM, Hoogvliet P, Randsdorp MS, Glerum S, van Middelkoop M, Koes BW. Carpal tunnel syndrome. Part I: effectiveness of nonsurgical treatments--a systematic review. Arch Phys Med Rehabil. 2010; 91:981–1004. [PubMed: 20599038]

Jessurun W, Hillen B, Zonneveld F, Huffstadt AJ, Beks JW, Overbeek W. Anatomical relations in the carpal tunnel: a computed tomographic study. J Hand Surg [Br]. 1987; 12:64–7.

Kamolz LP, Schrogendorfer KF, Rab M, Girsch W, Gruber H, Frey M. The precision of ultrasound imaging and its relevance for carpal tunnel syndrome. Surg Radiol Anat. 2001; 23:117–21. [PubMed: 11462859]

Kato T, Kuroshima N, Okutsu I, Ninomiya S. Effects of endoscopic release of the transverse carpal ligament on carpal canal volume. J Hand Surg [Am]. 1994; 19:416–9.

Kim DH, Marquardt TL, Gabra JN, Shen ZL, Evans PJ, Seitz WH, Li ZM. Pressure-morphology relationship of a released carpal tunnel. J Orthop Res. 2013 (in press).

Kline SC, Moore JR. The transverse carpal ligament. An important component of the digital flexor pulley system. J Bone Joint Surg Am. 1992; 74:1478–85. [PubMed: 1469007]

Lee CH, Kim TK, Yoon ES, Dhong ES. Postoperative morphologic analysis of carpal tunnel syndrome using high-resolution ultrasonography. Ann Plast Surg. 2005; 54:143–6. [PubMed: 15655463]

Li ZM, Masters TL, Mondello TA. Area and shape changes of the carpal tunnel in response to tunnel pressure. J Orthop Res. 2011; 29:1951–6. [PubMed: 21608024]

Li ZM, Tang J, Chakan M, Kaz R. Carpal tunnel expansion by palmarly directed forces to the transverse carpal ligament. J Biomech Eng. 2009; 131:081011. [PubMed: 19604023]

Mesgarzadeh M, Schneck CD, Bonakdarpour A. Carpal tunnel: MR imaging. Part I. Normal anatomy. Radiology. 1989a; 171:743–8. [PubMed: 2717746]

Mesgarzadeh M, Schneck CD, Bonakdarpour A, Mitra A, Conaway D. Carpal tunnel: MR imaging. Part II. Carpal tunnel syndrome. Radiology. 1989b; 171:749–54. [PubMed: 2541464]

Mogk JP, Keir PJ. Evaluation of the carpal tunnel based on 3-D reconstruction from MRI. J Biomech. 2007; 40:2222–9. [PubMed: 17166503]

Moore JS. Biomechanical models for the pathogenesis of specific distal upper extremity disorders. Am J Ind Med. 2002; 41:353–69. [PubMed: 12071489]

Okutsu I, Ninomiya S, Hamanaka I, Kuroshima N, Inanami H. Measurement of pressure in the carpal canal before and after endoscopic management of carpal tunnel syndrome. J Bone Joint Surg Am. 1989; 71:679–83. [PubMed: 2732256]

Pacek CA, Tang J, Goitz RJ, Kaufmann RA, Li ZM. Morphological Analysis of the Carpal Tunnel. Hand (N Y). 2010; 5:135–140. [PubMed: 19701670]

Richman JA, Gelberman RH, Rydevik BL, Gylys-Morin VM, Hajek PC, Sartoris DJ. Carpal tunnel volume determination by magnetic resonance imaging three-dimensional reconstruction. J Hand Surg [Am]. 1987; 12:712–7.

Richman JA, Gelberman RH, Rydevik BL, Hajek PC, Braun RM, Gylys-Morin VM, Berthoty D. Carpal tunnel syndrome: morphologic changes after release of the transverse carpal ligament. J Hand Surg [Am]. 1989; 14:852–7.

Sarria L, Cabada T, Cozcolluela R, Martinez-Berganza T, Garcia S. Carpal tunnel syndrome: usefulness of sonography. Eur Radiol. 2000; 10:1920–5. [PubMed: 11305571]

Seradge H, Jia YC, Owens W. In vivo measurement of carpal tunnel pressure in the functioning hand. J Hand Surg [Am]. 1995; 20:855–9.

Shen ZL, Li ZM. Ultrasound assessment of transverse carpal ligament thickness: a validity and reliability study. Ultrasound Med Biol. 2012; 38:982–8. [PubMed: 22502882]

Shen ZL, Li ZM. Biomechanical interaction between the transverse carpal ligament and the thenar muscles. J Appl Physiol. 2013; 114:225–227. [PubMed: 23221960]

Sora MC, Genser-Strobl B. The sectional anatomy of the carpal tunnel and its related neurovascular structures studied by using plastination. Eur J Neurol. 2005; 12:380–4. [PubMed: 15804269]

Tsujii M, Hirata H, Morita A, Uchida A. Palmar bowing of the flexor retinaculum on wrist MRI correlates with subjective reports of pain in carpal tunnel syndrome. J Magn Reson Imaging. 2009; 29:1102–5. [PubMed: 19388125]

Tung WL, Zhao C, Yoshii Y, Su FC, An KN, Amadio PC. Comparative study of carpal tunnel compliance in the human, dog, rabbit, and rat. J Orthop Res. 2010; 28:652–6. [PubMed: 19918895]

Uchiyama S, Itsubo T, Yasutomi T, Nakagawa H, Kamimura M, Kato H. Quantitative MRI of the wrist and nerve conduction studies in patients with idiopathic carpal tunnel syndrome. J Neurol Neurosurg Psychiatry. 2005; 76:1103–8. [PubMed: 16024888]

Viegas SF, Pollard A, Kaminksi K. Carpal arch alteration and related clinical status after endoscopic carpal tunnel release. J Hand Surg [Am]. 1992; 17:1012–6.

Xiu KH, Kim JH, Li ZM. Biomechanics of the transverse carpal arch under carpal bone loading. Clin Biomech (Bristol, Avon). 2010; 25:776–80.

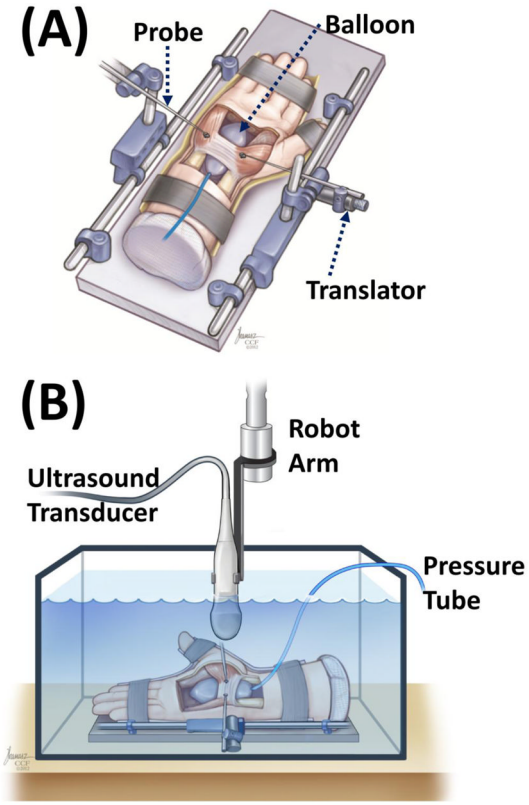

Figure 1.
Experimental setup for carpal arch width narrowing (A) and ultrasound imaging (B)

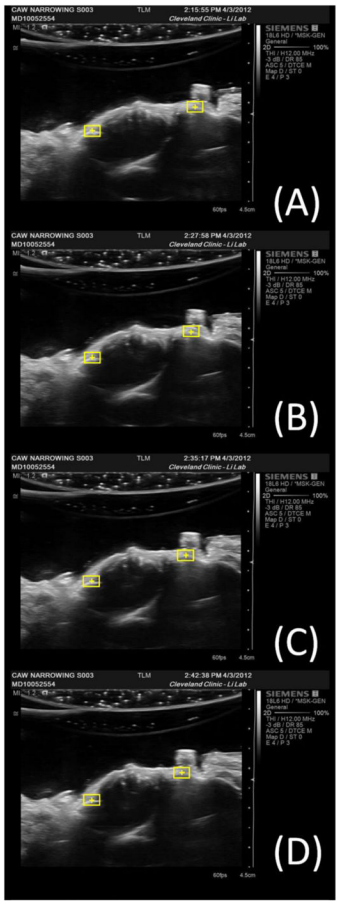

Figure 2.
Ultrasound images of a representative specimen at (a) its initial CAW of 26.7 mm, (b) 1 mm narrowing of the CAW, (c) 2 mm narrowing of the CAW, and (d) 3 mm narrowing of the CAW. The yellow boxes are the regions of interest with their centroids at the most palmar aspect of the hamate and the trapezium.

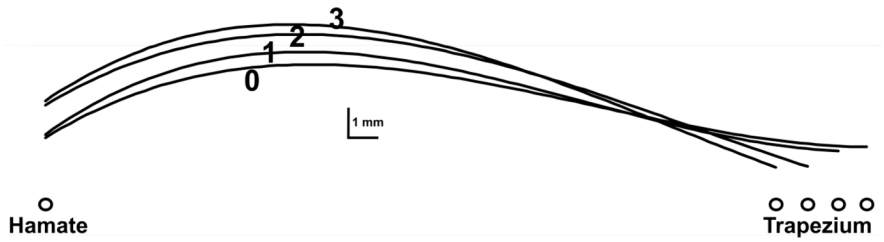

Figure 3.
Representative curves of the transverse carpal ligament at different CAWs. The labels 0, 1, 2 and 3 indicate conditions of CAW narrowing of 0, 1, 2 and 3 mm, respectively.

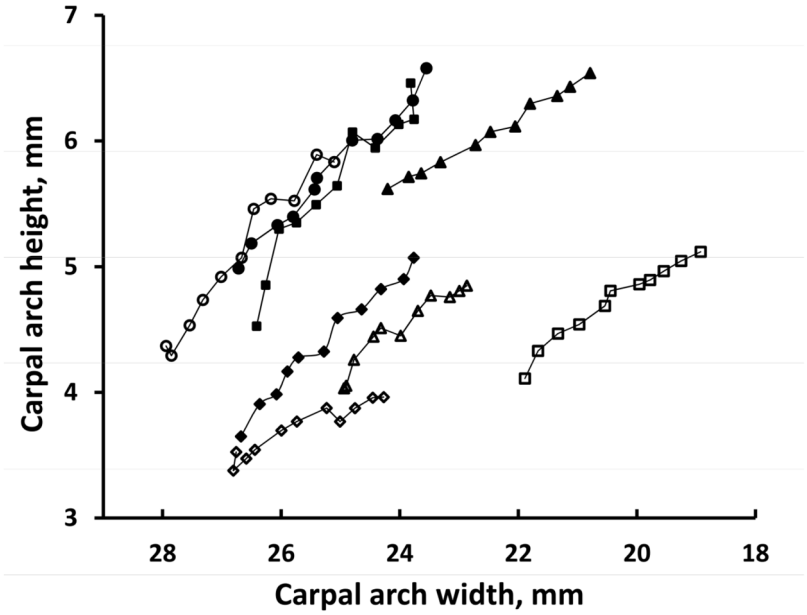

Figure 4.
Carpal arch heights at different carpal arch widths for individual specimens.

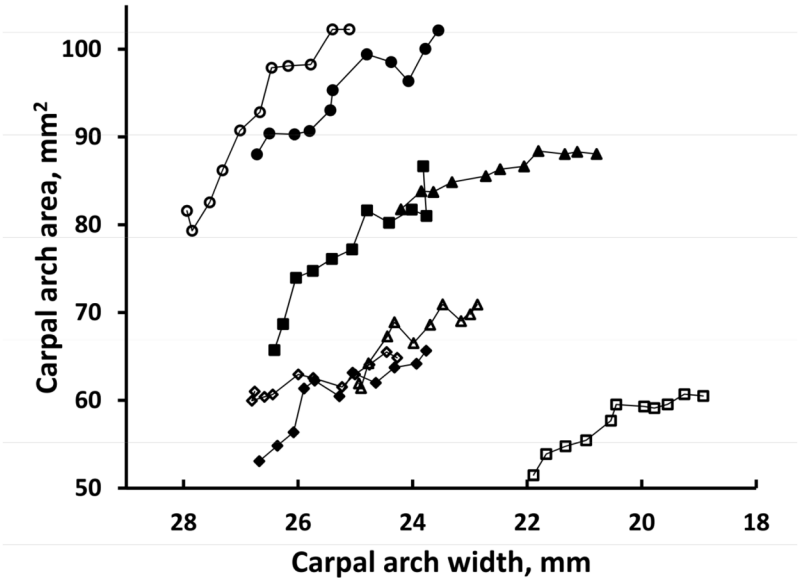

Figure 5.
Carpal arch areas at different carpal arch widths for individual specimens.

Table 1

Linear regression of the CAH and the CAA as a function of the CAW.

	CAH			CAA		
Specimen	***a***	***b***	R^2	***a***	***b***	R^2
1	−0.578	19.620	0.906	−5.765	221.565	0.854
2	−0.313	10.600	0.963	−2.929	117.184	0.893
3	−0.456	16.718	0.981	−4.069	197.205	0.884
4	−0.581	20.107	0.957	−8.412	316.270	0.935
5	−0.451	15.275	0.977	−3.665	153.175	0.784
6	−0.206	8.501	0.915	−1.793	108.375	0.825
7	−0.269	11.615	0.991	−1.828	127.055	0.920
8	−0.362	12.691	0.908	−3.801	158.308	0.759
Average	−0.402	14.391	0.950	−4.033	174.892	0.857
SD	0.138	4.240	0.035	2.187	69.131	0.063

Note: *a* and *b* are the coefficients of the regression equation $y = ax + b$, where *x* is for the CAW and *y* represents the CAH or the CAA. The R^2-value is the coefficient of determination indicating the goodness of the linear fit.